Engineering Applications of Computational Fluid Mechanics ›
Volume 13, 2019 - Issue 1

Articles

Applicability of connectionist methods to predict dynamic viscosity of silver/water nanofluid by using ANN-MLP, MARS and MPR algorithms

Mohammad Hossein Ahmadi, Behnam Mohseni-Gharyehsafa, Mahmood Farzaneh-Gord, Ravindra D. Jilte, Ravinder Kumar & Kwok-wing Chau

Pages 220-228 | Received 02 Dec 2018, Accepted 15 Jan 2019, Published online: 05 Mar 2019

Cite this article https://doi.org/10.1080/19942060.2019.1571442

ABSTRACT

Dynamic ... Due to
improve ... ese types of
fluids ar ... scosity
relies on
temp ... polynomial
regre ... and
multivar ... ynamic
viscosity ... estigations
are emp ... deling
process ... rature and

models are 0.9998, 0.9997 and 0.9996 for the ANN-MLP, MARS and MPR algorithms, respectively. In addition, based on importance analysis, the temperature is highly effective and the dominant parameter for the dynamic viscosity of the nanofluid in comparison with size and concentration.

KEYWORDS: nanofluid dynamic viscosity artificial neural network concentration multivariate adaptive regression splines (MARS) multivariable polynomial regression (MPR)

Nomenclature

φ	=	Concentration
T	=	Temperature (°C)
d	=	Size (nm)
μ	=	Dynamic viscosity
ai		
bi		
BF		
GCV		
AAPRE		

In this article

RMSE	=	Root mean square error
R2	=	Coefficient of determination
MARS	=	Multivariate adaptive regression splines
MPR	=	Multivariable polynomial regression
ANN	=	Artificial neural network
MLP	=	Multilayer perceptron
C(M)	=	Complexity penalty

1. Introduction

Nano-siz … l in a base
fluid to p … Nazari,
Ghasem … e,
nanoflui … used in
various … eating, etc.
More … al systems
to en … & Chau,
2019; Sa … Wang & Jiao,
2015). T … hese
material … ity. Adding
nanostru … heat, etc.

temperature, synthesis procedure, pH and concentration is investigated in several pieces of research (Baghban, Jalali, Shafiee, Ahmadi, & Chau, 2019; Hosseini, Kasaeian, Pourfayaz, Sheikhpour, & Wen, 2018; Zeinali Heris, Kazemi-Beydokhti, Noie, & Rezvan, 2012).

The dynamic viscosity of nanofluids significantly affects their fluid flow and heat transfer (Ahmadi et al., 2018; Ebrahimi-Moghadam, Mohseni-Gharyehsafa, & Farzaneh-Gord, 2018; Mohseni-Gharyehsafa et al., 2018; Nazari, Ahmadi, Ghasempour, & Shafii, 2018). Given this fact, it is critical to get better awareness of the parameters affecting this property. According to the literature review, an increase in temperature results in lower dynamic viscosity, which facilitates fluid motion due to the reduction in friction. Another effective factor in dynamic viscosity is the concentration of nanostructures dispersed in the base fluid (Chiam, Azmi, Usri, Mamat, & Adam, 2017; Soltani & Akbari, 2016). On the basis of the results of experimental studies, an increase in concentration leads to an improvement of dynamic viscosity (Asadi & Asadi, 2016). The size of nanostructures plays a key role in thermophysical properties of nanofluids.

Artificial neural networks are widely employed for modeling the system and pattern recognition. Artificial neural networks are applicable in modeling the thermophysical properties of nanofluids (Ahmadi, Tatar, Nazari, Mahian, & Ghasempour, 2018; Chau, 2017; Kazemi et al., 2018; Rezaei, Sadeghzadeh, Alhuyi Nazari, Ahmadi, & Astaraei, 2018). Ahmadi et al. (2018) employed the least square support vector machine (LSSVM) and group method of data handling (GMDH) approaches to model the thermal conductivity value of CuO/EG (Copper-Oxide/Ethylene-Glycol) nanofluid. It was
monitore … e equal to
0.994 ar … the models
in estima … rch (Ahmadi
et al., 20 … umina/EG.
The R^2 v … Baghban et
al. (201 … oefficients of
the c … dependent
paramet … Statistical
criteria s … highest
accuracy

To propo … ng the

concentration when modeling thermophyscial properties; adding size as another input variable results in more accurate results. In the current study, the Ag/water nanofluid's dynamic viscosity is modeled by applying MPR, ANN-MLP and MARS algorithms. The input variables in the modeling process are temperature, size and volumetric concentration.

---

2. Intelligent modes

2.1. Multilayer perceptron neural network

Artificial neural networks are conventionally applied for prediction purposes. MLP is a feed-forward neural network algorithm. This network is composed of an input layer, hidden layer and output layer (Gardner & Dorling, 1998; Hornik, Stinchcombe, & White, 1989). The number of input and output layers depends on the data. In the hidden layer, one or more layers can exist that have various neurons (Orhan, Hekim, & Ozer, 2011). In these types of neural networks, the initial neuron of the layer is fed into the neuron of layer in the next stage, which is the same for all layers except the first layer. Each neuron has an activation function and a sum function. The inputs are initially multiplied by the weighting factor and added to each other. Afterwards, a bias factor is added to the calculated number. In the next step, the number obtained from the summing function is used in the activation function as input data. Activation functions are categorized in three forms as represented below, where ϕ is the activation function (Ruck, Rogers, Kabrisky, Oxley, & Suter, 1990; Vanzella et al., 2004).

$\varphi(r)=\exp$ ... s the interpola ... is defined by r.

Trial and ... calculate the num ... n Square Error ... ideal status of bias a ... results, an accurate ... & Sayyouh, 2003).

2.2. Mu

In this article

MARS is applied in regression and data classification (Friedman & Roosen, 1995). This approach is mainly utilized to predict the dependent data, Y ($n \times 1$), which are continuous, based on the group of input data ($n \times p$). This model is represented as follows:

$$y = f(x) + e \quad (2)$$

In the above equation, f indicates the weighted sum of basic functions. These functions are dependent on X. In addition, e stands for the error, which is an ($n \times 1$) matrix. In this method, no priori assumption is required for estimating the relationship between dependent and independent data. The relationship between these data is found on the basis of a group of coefficients and piecewise polynomials. The model is generated using this algorithm based on fitting basic functions to independent variables' distinct intervals. Typically, the polynomials that are called "splines" consist of pieces connecting to each other. The connecting points of the splines are known as "nodes," "knots" or "breakdown points." The points are shown by t. In a q-degree spline, each section is a polynomial function. The function utilized by the MARS algorithm is described as:

$$[-(x-t)]_+^q = \begin{cases} (t-x)^q & \text{if } x < t \\ 0 & \text{otherwise} \end{cases} \quad (3)$$

$$[+(x-t)]_+^q = \begin{cases} (t-x)^q & \text{if } x \geq t \\ 0 & \text{otherwise} \end{cases} \quad (4)$$

In the above equation, q (≥ 0) is the power at which the splines are boosted up. The smoothness of the obtained function depends on the value of q. In the case of $q = 1$, as in the present study, just simple linear splines are applied. In Figure 1, a pair of splines for the node $t = 3.5$ is shown.

Figure 1. … endez

Fernand…

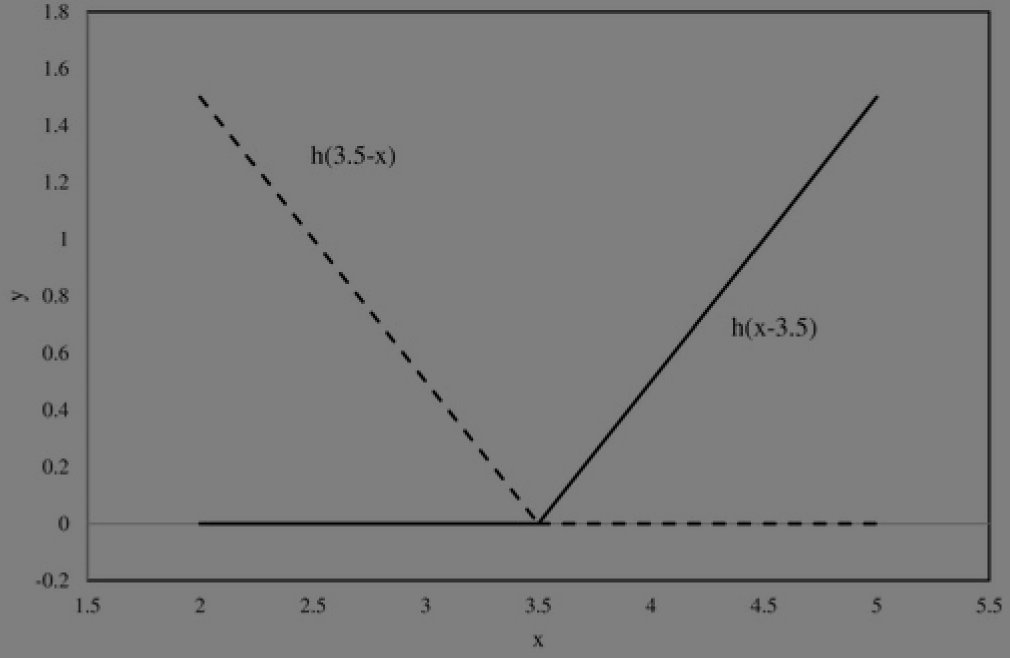

Display full size

By considering y which has M bias functions, the model proposed by MARS can be written (Chou, Lee, Shao, & Chen, 2004; De Cos Juez, Lasheras, García Nieto, & Suárez, 2009; Friedman & Roosen, 1995; Nieto & Antón, 2014; Nieto, Fernández, Lasheras, de Cos Juez, & Muñiz, 2012; Nieto, Lasheras, de Cos Juez, & Fernández, 2011; Orhan et al., 2011; Xu et al., 2004) as:

$$\hat{y}=\hat{f}_M(x)=c_0+\sum_{m=1}^{M}c_mB_m(x) \quad (5)$$

$\hat{y}$ indicates the parameter predicted by MARS, c_0 is a fixed value, the mth bias function is referred to as $B_m(x)$ and c_m refers to the mth basic function's coefficient. It is crucial to optimize the variables (c_0 and c_m) announced into the knot positions and the model. For a dataset of X which has n objects and p input variables, $N = n \times p$ pairs of spline basic functions exist which can be calculate[illegible] a two-step

process [illegible] se process is

perform[illegible] al., 2009;

Friedma[illegible] al., 2011;

Orhan et [illegible] to a model

with ina[illegible] erfitting of

the [illegible] ay be

remove[illegible] usable

function[illegible] man &

Roosen, [illegible] 011; Xu et

al., 2004 [illegible] dual error

divided [illegible] ulated as

$$GCV(M)=\frac{1}{n}\sum_{i=1}^{n}\frac{(y_i-\hat{f}_M(x_i))^2}{(1-C(M)/n)^2} \quad (6)$$

C(M) refers to complexity penalty, which depends on the number of basic functions and can be obtained (Chou et al., 2004; De Cos Juez et al., 2009; Friedman & Roosen, 1995; Nieto & Antón, 2014; Nieto et al., 2012, 2011; Orhan et al., 2011; Xu et al., 2004) as: $C(M)=(M+1)+dM$ (7) M refers to the number of functions used as basic in Equation (5); d indicates a penalty for the basic functions utilized in the proposed model. Increase in the value of d causes fewer required basic functions and smoother estimation.

When the MARS model is generated, the importance of the utilized variables for modeling can be assessed. Taking into account the literatures several criteria can be applied which in this study, the GCV parameter is used for this purpose to achieve reliable results (Chou et al., 2004; De Cos Juez et al., 2009; Friedman & Roosen, 1995; Nieto & Antón, 2014; Nieto et al., 2012, 2011; Orhan et al., 2011; Xu et al., 2004).

3. Results and discussion

3.1. Multivariable polynomial regression

In this study, experimental results from previous publications are used to model the range of the input variables and represented in Table 1. The data used for the modeling step are taken from experiments that were published recently (Alade, Oyehan, Popoola, Olatunji, & Bagudu, 2018; Esfe, Saedodin, Biglari, & Rostamian, 2016; Nikkam & Toprak, 2018). The temperature of the fluid and the concentration ratio of the Ag/water nanoflui … dynamic viscosity …

Figure 2. … ure.

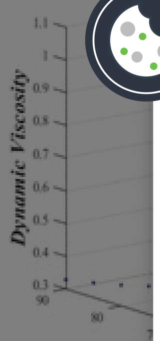

Table 1. Ranges of input variables (Alade et al., 2018 ; Esfe et al., 2016 ; Nikkam & Toprak, 2018)

By using 2D multivariate polynomial regression and applying the least square method (Royston & Sauerbrei, 2008; Sinha, 2013), a simple equation is obtained for the experimental data that is represented in Alade et al. (2018), Esfe et al. (2016) and Nikkam and Toprak (2018). The proposed model has three inputs including temperature, size of nanoparticles and volumetric concentration. This model is very simple, lacking any exponential or logarithmic term. The complex models obtained by neural networks have some disadvantages such as high computational cost. The coefficients of the model are shown in Equation (8):

$$\mu = a_1 + a_2\times T + a_3\times\varphi + a_4\times d + a_5\times T\times\varphi + a_6\times d\times T + a_7\times d\times\varphi + a_8\times\varphi^2 + a_9\times T^2 \quad (8)$$

3.2. Multivariate adaptive regression splines

As mentioned earlier, in the MARS algorithm, the cores of procedure are basic functions; therefore, it is necessary to choose appropriate ones. Unlimited increase in the basic functions causes overfitting. In this study, the sensitivity of the MARS model based on the input basic functions is investigated. According to Jerome H. Friedman (1991), the GCV method is used to obtain the optimal number of functions in which using 10 … s of the propose…

Figure 3.

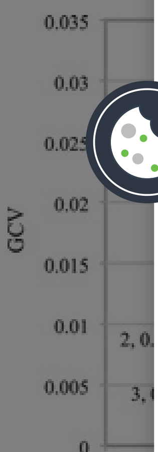

Display full size

Table 2. Coefficients of the proposed models

Display Table

The model obtained using 10 basic functions is represented in Equation (9). The coefficients of the proposed model in Equation (9) are reported in Table 2.

$$\mu = b7 + b8\times BF1 + b9\times BF2 + b10\times BF3 + b11\times BF4 + b12\times BF5 + b13\times BF6 + b14\times BF7 + b15\times BF8 + b16\times BF9 + b17\times BF10 \quad (9)$$

$$BF1=\mathrm{Max}(0,T-b1); BF2=\mathrm{Max}(0,b1-T) BF3=\mathrm{Max}(0,\varphi-b2); BF4=\mathrm{Max}(0,b2-\varphi) BF5=\mathrm{Max}(0,b3-d); BF6=\mathrm{Max}(0,b4-T) BF7=BF5\times \mathrm{Max}(0,b2-\varphi); BF8=BF1\times \mathrm{Max}(0,\varphi-b5) BF9=BF1\times \mathrm{Max}(0,b5-\varphi); BF10=BF4\times \mathrm{Max}(0,b6-T)$$

In most of the studies in which the MARS method is used for regression modeling, the importance of data is calculated for gaining better insight into the influential parameters. Data whose importance is equal to 0 will be removed.

In order for gaining the relative importance of one parameter, the root square of the GCV of the all basis function without involving the propsed parameter should be obtain and then the value must be scaled to 100. Based on importance data analysis, temperature has the most significant effect compared with temperature and concentration (Figure 4). The concentration of nanofluid has the second rank in the calculation of dynamic viscosity.

Figure 4.

In this article

3.3. MLP-LMA: feed-forward back propagation with Levenberg–Marquardt training Algorithm

In MLP neural networks, hidden layers and their neurons play the key role in regression. Inappropriate model selection and an inadequate number of layers and neurons lead to unfavorable outputs. Therefore, it is necessary analyze the sensitivity of the network to the number of neurons and hidden layers. Since there are three input variables, a hidden layer is appropriate to obtain acceptable training; however, the sensitivity of the network must be considered based on the number of neurons. In the present study, MSE is used as criterion to select the optimum number of neurons. As shown in Figure 5 , using neurons leads to the best model.

Figure 5. MSE value for various number of neurons.

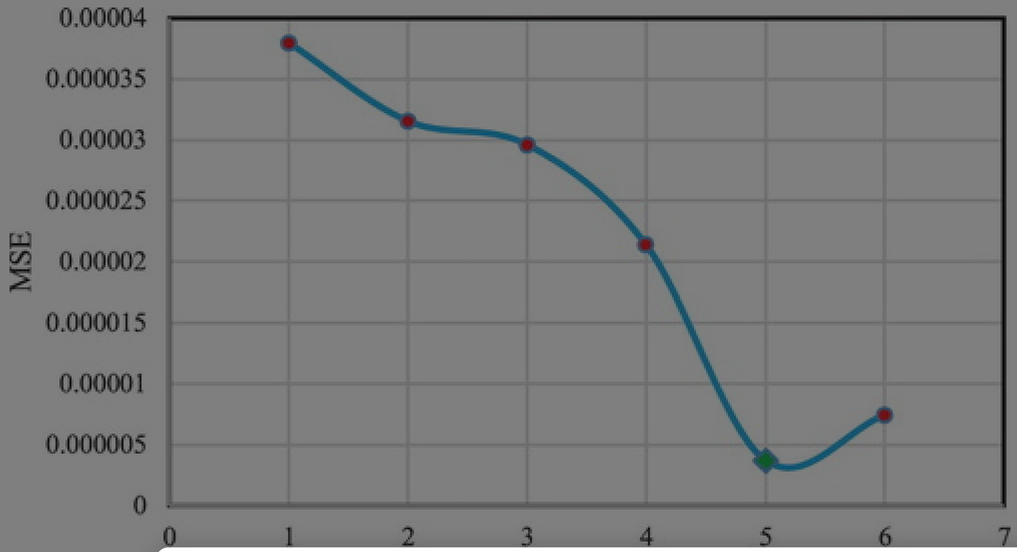

Neural N ... 15% for
validatio ... for the
hidden ... yer. The
best ... gures 6 and
7 are rep ... on the
concentr ... of Ag/water
nanoflui ... .009 and
0.012 in ... les in these

In this article

dynamic viscosity for each temperature. In addition, it can be concluded that higher temperature causes lower dynamic viscosity for a constant concentration. For instance, increasing the temperature from 50 to 70°C in 0.003 concentration leads to approximately 19.5% reduction in dynamic viscosity.

Figure 6 Dynamic viscosity of Ag/water nanofluid in different temperatures and concentrations.

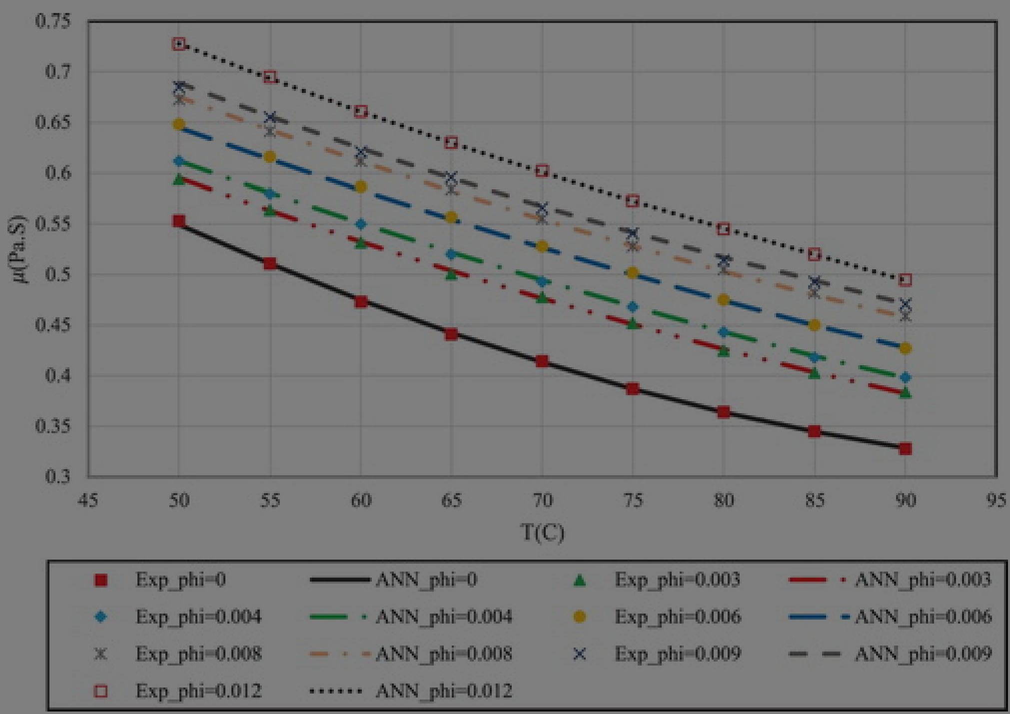

Display full size

Figure 7. Dynamic viscosity of Ag/water nanofluid versus temperature and concentration.

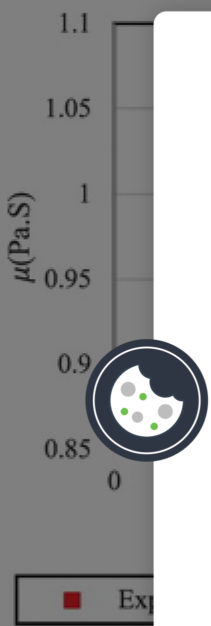

Display full size

In this article

In Figure 7 is represented the dynamic viscosity of Ag/water nanofluid in 20 and 25°C for particle size equal to 40 nm. The concentrations of the solid phase in these conditions are in the range of 0.00096 and 0.01. As illustrated, an increase in concentration, with constant temperature and particle size, results in improvement in dynamic viscosity; while a temperature increase reduces the dynamic viscosity.

3.4. Statistical comparison of the proposed models

AAPRE%=∑i=1nti−oitin×100(Average Absolute Percent Relative Error)

RMSE=1n∑i=1n(ti−oi)212(Root Mean Square Error)

R2=1−∑i=1n(ti−oi)∑i=1n(ti−tm),tm=∑i=1ntin(Coefficient of determination)

Based on the statistical criteria for regression evaluation (Baghban, Kahani, Nazari, Ahmadi, & Yan, 2019; Hajikhodaverdikhan, Nazari, Mohsenizadeh, Shamshirband, & Chau, 2018; Taormina, Chau, & Sivakumar, 2015; Wu & Chau, 2011), the MLP network is the best among the approaches represented in the present study for modeling the dynamic viscosity of Ag/water nanofluid; however, using this algorithm requires more computational cost than does polynomial regression. A summary of the results obtained for each algorithm is presented in Table 3.

Table 3. Statistical comparison of various models

Display Table

4. Con

In the pr ... the
dynamic ... and
concent ... of R^2 was
used ... ing to the
calculat ... ual to
0.9998, ... istical
criterias ... ther
algorith ... riate for
modelin ... id. In

In this article

into the influential factors. Based on the obtained values, the importance of temperature, concentration and size was approximately 100%, 80% and 12%, respectively. These values indicate the high importance of temperature in modeling the dynamic viscosity.

Disclosure statement

No potential conflict of interest was reported by the authors.

Related Research Data

Rainfall–runoff modeling using artificial neural network coupled with singular spectrum analysis
Source: Elsevier BV
Study of cyanotoxins presence from experimental cyanobacteria concentrations using a new data mining methodology based on multivariate adaptive regression splines in Trasona reservoir (Northern Spain).
Source: Elsevier BV
Fabrication and thermo-physical characterization of silver nanofluids: An
expe
Sour
Apply ... our
nord
Sour
O
So
Appli
pulsa
Sour
Mode ... e

Source: Elsevier BV
Developing an ANFIS-based swarm concept model for estimating the relative viscosity of nanofluids
Source: Informa UK Limited
Novel genetic-based negative correlation learning for estimating soil temperature
Source: Taylor & Francis Group
Multivariable Model-Building
Source: John Wiley & Sons, Ltd
Dynamic viscosity of MWCNT/ZnO–engine oil hybrid nanofluid: An experimental investigation and new correlation in different temperatures and solid concentrations
Source: Elsevier BV
Multivariate Adaptive Regression Splines
Source: Institute of Mathematical Statistics
Thermal conductivity and dynamic viscosity modeling of Fe2O3/water nanofluid by applying various connectionist approaches
Source: Informa UK Limited
Earthquake prediction with meteorological data by particle filter-based support vector regression
Source: Informa UK Limited
Multivariate adaptive regression splines—studies of HIV reverse transcriptase inhibitors
Sour
Rigo ... ed with
evol
Sour
A ne ... e of
diet ... sal
w
Sou
Expe
enha
Sour
Mixe

Source: International Information and Engineering Technology Association

Photometric redshifts with the Multilayer Perceptron Neural Network: application to the HDF-S and SDSS

Source: EDP Sciences

An experimental study on thermophysical properties and heat transfer characteristics of low volume concentrations of Ag-water nanofluid☆

Source: Elsevier BV

Experimental and numerical analysis of a nanofluidic thermosyphon heat exchanger

Source: Informa UK Limited

Novel ZnO-Ag/MWCNT nanocomposite for the photocatalytic degradation of phenol

Source: Elsevier

Effects of temperature and particles concentration on the dynamic viscosity of MgO-MWCNT/ethylene glycol hybrid nanofluid: Experimental study

Source: Elsevier BV

Tool wear prediction in hard turning of EN8 steel using cutting force and surface roughness with artificial neural network

Source: SAGE Publications

Thermal conductivity and viscosity of Al2O3 nanofluids for different based ratio of water and ethylene glycol mixture

Source: Elsevier BV

AN INTRODUCTION TO MULTIVARIATE ADAPTIVE REGRESSION SPLINES

Determination of thermal conductivity ratio of CuO/ethylene glycol nanofluid by connectionist approach
Source: Elsevier BV
Application of ANFIS and LSSVM strategies for estimating thermal conductivity enhancement of metal and metal oxide based nanofluids
Source: Informa UK Limited
Mining the breast cancer pattern using artificial neural networks and multivariate adaptive regression splines
Source: Elsevier BV
Artificial neural networks (the multilayer perceptron)—a review of applications in the atmospheric sciences
Source: Elsevier BV
Connectionist intelligent model estimates of convective heat transfer coefficient of nanofluids in circular cross-sectional channels
Source: Springer Science and Business Media LLC
How to improve the thermal performance of pulsating heat pipes: A review on working fluid
Source: Elsevier BV
Neural network river forecasting through baseflow separation and binary-coded swarm optimization
Source: Elsevier BV
A review of thermal conductivity of various nanofluids
Source: Elsevier BV
A RE
Sour
Preci ... glycol–
wate
Sour
Sens ... dict the
h
Sou
Multi
Sour
Usin ... ntropy
gene ... ollector

References

1. Ahmadi, M.-A., Ahmadi, M. H., Alavi, M. F., Nazemzadegan, M. R., Ghasempour, R., & Shamshirband, S. (2018). Determination of thermal conductivity ratio of CuO/ethylene glycol nanofluid by connectionist approach. Journal of the Taiwan Institute of Chemical Engineers, 91, 383–395.
   Web of Science ® | Google Scholar

2. Ahmadi, M. H., Ahmadi, M. A., Nazari, M. A., Mahian, O., & Ghasempour, R. (2018). A proposed model to predict thermal conductivity ratio of Al 2 O 3/EG nanofluid by applying least squares support vector machine (LSSVM) and genetic algorithm as a connectionist approach. Journal of Thermal Analysis and Calorimetry, 1–11.
   Web of Science ® | Google Scholar

3. Ahmadi, M. H., Mirlohi, A., Nazari, M. A., & Ghasempour, R. (2018). A review of thermal conductivity of various nanofluids. Journal of Molecular Liquids, 265, 181–188.
   Web of Science ® | Google Scholar

4. Ahmadi, M. H., Tatar, A., Nazari, M. A., Ghasempour, R., Chamkha, A. J., & Yan, W.-M.
   (2018 … ce of
   pulsat … Journal of
   Heat a

5. Ah … heremet, M.
   A. (… 3/water
   nanof … Transfer,
   Part A

6. Alade, I. O., Oyehan, T. A., Popoola, I. K., Olatunji, S. O., & Bagudu, A. (2018). Modeling thermal conductivity enhancement of metal and metallic oxide nanofluids using support vector regression. Advanced Powder Technology, 29(1), 157–167.
Web of Science ® | Google Scholar

7. Asadi, M., & Asadi, A. (2016). Dynamic viscosity of MWCNT/ZnO–engine oil hybrid nanofluid: An experimental investigation and new correlation in different temperatures and solid concentrations. International Communications in Heat and Mass Transfer, 76, 41–45.
Web of Science ® | Google Scholar

8. Baghban, A., Jalali, A., Shafiee, M., Ahmadi, M. H., & Chau, K.-W. (2019). Developing an ANFIS-based swarm concept model for estimating the relative viscosity of nanofluids. Engineering Applications of Computational Fluid Mechanics, 13(1), 26–39.
Web of Science ® | Google Scholar

9. Baghban, A., Kahani, M., Nazari, M. A., Ahmadi, M. H., & Yan, W.-M. (2019). Sensitivity analysis and application of machine learning methods to predict the heat transfer performance of CNT/water nanofluid flows through coils. International Journal of Heat and Mass Transfer, 128, 825–835.
Web of Science ® | Google Scholar

10. Baghban, A., Pourfayaz, F., Ahmadi, M. H., Kasaeian, A., Pourkiaei, S. M., & Lorenzini, G. (20 ... ansfer coeffic ... ermal Analys

11. Ch ... delling. Mu
Goog

12. Chiam ... ductivity and vi ... thylene

In this article

Web of Science ® | Google Scholar

13. Chou, S.-M., Lee, T.-S., Shao, Y. E., & Chen, I.-F. (2004). Mining the breast cancer pattern using artificial neural networks and multivariate adaptive regression splines. Expert Systems with Applications, 27(1), 133–142.
Web of Science ® | Google Scholar

14. De Cos Juez, F. J., Lasheras, F. S., García Nieto, P. J., & Suárez, M. S. (2009). A new data mining methodology applied to the modelling of the influence of diet and lifestyle on the value of bone mineral density in post-menopausal women. International Journal of Computer Mathematics, 86(10-11), 1878–1887.
Web of Science ® | Google Scholar

15. Ebrahimi-Moghadam, A., Mohseni-Gharyehsafa, B., & Farzaneh-Gord, M. (2018). Using artificial neural network and quadratic algorithm for minimizing entropy generation of Al 2 O 3-EG/W nanofluid flow inside parabolic trough solar collector. Renewable Energy, 129, 473–485.
Web of Science ® | Google Scholar

16. Esfe, M. H., Saedodin, S., Biglari, M., & Rostamian, H. (2016). An experimental study on thermophysical properties and heat transfer characteristics of low volume concentrations of Ag-water nanofluid. International Communications in Heat and Mass Transfer, 74, 91–97.

17. Friedn ... ls of
Statist

18. Frie ... aptive
regres

19. Gardn ... ayer

Environment, 32(14-15), 2627–2636.
| Web of Science ® | Google Scholar

20. Goda, H. M., Shokir, E.-M., Eissa, M., Fattah, K. A., & Sayyouh, M. H. (2003). Prediction of the PVT data using neural network computing theory. Nigeria annual international conference and exhibition.
Google Scholar

21. Hajikhodaverdikhan, P., Nazari, M., Mohsenizadeh, M., Shamshirband, S., & Chau, K.-W. (2018). Earthquake prediction with meteorological data by particle filter-based support vector regression. Engineering Applications of Computational Fluid Mechanics, 12(1), 679–688.
| Web of Science ® | Google Scholar

22. Hornik, K., Stinchcombe, M., & White, H. (1989). Multilayer feedforward networks are universal approximators. Neural Networks, 2(5), 359–366.
| Web of Science ® | Google Scholar

23. Hosseini, F., Kasaeian, A., Pourfayaz, F., Sheikhpour, M., & Wen, D. (2018). Novel ZnO-Ag/MWCNT nanocomposite for the photocatalytic degradation of phenol. Materials Science in Semiconductor Processing, 83, 175–185.
| Web of Science ® | Google Scholar

24. Kazem M. A., Chau, K.-W., learning for estima luid Mecha

25. Mo rd, M., Ahma ifferent nanofl n approach. Journa
Web

26. Nazari, M. A., Ahmadi, M. H., Ghasempour, R., & Shafii, M. B. (2018). How to improve the thermal performance of pulsating heat pipes: A review on working fluid. Renewable and Sustainable Energy Reviews, 91, 630–638.
Web of Science ® | Google Scholar

27. Nazari, M. A., Ghasempour, R., Ahmadi, M. H., Heydarian, G., & Shafii, M. B. (2018). Experimental investigation of graphene oxide nanofluid on heat transfer enhancement of pulsating heat pipe. International Communications in Heat and Mass Transfer, 91, 90–94.
Web of Science ® | Google Scholar

28. Nieto, P. G., & Antón, JÁ. (2014). Nonlinear air quality modeling using multivariate adaptive regression splines in Gijón urban area (Northern Spain) at local scale. Applied Mathematics and Computation, 235, 50–65.
Web of Science ® | Google Scholar

29. Nieto, P. G., Fernández, J. A., Lasheras, F. S., de Cos Juez, F., & Muñiz, C. D. (2012). A new improved study of cyanotoxins presence from experimental cyanobacteria concentrations in the Trasona reservoir (Northern Spain) using the MARS technique. Science of the Total Environment, 430, 88–92.
PubMed | Web of Science ® | Google Scholar

30. Nieto, P. G., García-Gonzalo, E., Bernardo Sanchez, A., & Menendez Fernandez, M.
(2016 … adaptive
regres … craft
engine
Web

31. Nie … dy of
cy … sing a new
data … es in
Trasor … 14–421.

In this article

32. Nikkam, N., & Toprak, M. S. (2018). Fabrication and thermo-physical characterization of silver nanofluids: An experimental investigation on the effect of base liquid. International Communications in Heat and Mass Transfer, 91, 196–200.
Web of Science ® | Google Scholar

33. Orhan, U., Hekim, M., & Ozer, M. (2011). EEG signals classification using the K-means clustering and a multilayer perceptron neural network model. Expert Systems with Applications, 38(10), 13475–13481.
Web of Science ® | Google Scholar

34. Ramezanizadeh, M., Alhuyi Nazari, M., Ahmadi, M. H., & Chau, K.-W. (2019). Experimental and numerical analysis of a nanofluidic thermosyphon heat exchanger. Engineering Applications of Computational Fluid Mechanics, 13(1), 40–47.
Web of Science ® | Google Scholar

35. Rezaei, M. H., Sadeghzadeh, M., Alhuyi Nazari, M., Ahmadi, M. H., & Astaraei, F. R. (2018). Applying GMDH artificial neural network in modeling CO2 emissions in four nordic countries. International Journal of Low-Carbon Technologies, 13(3), 266–271.
Web of Science ® | Google Scholar

36. Royston, P., & Sauerbrei, W. (2008). Multivariable model-building: A pragmatic approach to regression anaylsis based on fractional polynomials for modelling continuous variables (Vol. 777). London: John Wiley & Sons.

37. Ruck, ...). The multil... nt function. IEEE T...

38. Saidu... nd challe... (3), 1646–1668.

In this article

39. Sinha, P. (2013). Multivariate polynomial regression in data mining: Methodology, problems and solutions. International Journal of Scientific and Engineering Research, 4(12), 962–965.
Google Scholar

40. Soltani, O., & Akbari, M. (2016). Effects of temperature and particles concentration on the dynamic viscosity of MgO-MWCNT/ethylene glycol hybrid nanofluid: Experimental study. Physica E: Low-Dimensional Systems and Nanostructures, 84, 564–570.
Web of Science ® | Google Scholar

41. Taormina, R., Chau, K.-W., & Sivakumar, B. (2015). Neural network river forecasting through baseflow separation and binary-coded swarm optimization. Journal of Hydrology, 529, 1788–1797.
Web of Science ® | Google Scholar

42. Vanzella, E., Cristiani, S., Fontana, A., Nonino, M., Arnouts, S., Giallongo, E., … Zaggia, S. (2004). Photometric redshifts with the multilayer perceptron neural network: Application to the HDF-S and SDSS. Astronomy & Astrophysics, 423(2), 761–776.
Web of Science ® | Google Scholar

43. Vasanthakumari, R., & Pondy, P. (2018). Mixed convection of silver and titanium dioxide nanofluids along inclined stretching sheet in presence of MHD with heat generation and suction effect. Mathematical Modelling of Engineering Problems, 5(2), 123–1

44. Wang, … of heat pipe contai… ional Journal of …

45. Wu, C… network couple… 394–409.

46. Xu, Q.-S., Daszykowski, M., Walczak, B., Daeyaert, F., De Jonge, M., Heeres, J., … Massart, D. L. (2004). Multivariate adaptive regression splines—studies of HIV reverse transcriptase inhibitors. Chemometrics and Intelligent Laboratory Systems, 72(1), 27–34.

Web of Science ® | Google Scholar

47. Zeinali Heris, S., Kazemi-Beydokhti, A., Noie, S., & Rezvan, S. (2012). Numerical study on convective heat transfer of Al2O3/water, CuO/water and Cu/water nanofluids through square cross-section duct in laminar flow. Engineering Applications of Computational Fluid Mechanics, 6(1), 1–14.

Web of Science ® | Google Scholar